HHS Public Access

Author manuscript

Cell Rep. Author manuscript; available in PMC 2017 January 06.

Published in final edited form as:

Cell Rep. 2017 January 03; 18(1): 198–212. doi:10.1016/j.celrep.2016.11.083.

Opposing functions of microglial and macrophagic TNFR2 in the pathogenesis of experimental autoimmune encephalomyelitis

Han Gao[1,2], **Matt C. Danzi**[1,2,3], **Claire S. Choi**[4], **Mehran Taherian**[1], **Camilla Dalby-Hansen**[1,5], **Ditte G. Ellman**[5], **Pernille M. Madsen**[1,5], **John L. Bixby**[1,2,3,6], **Vance P. Lemmon**[1,2,3], **Kate L. Lambertsen**[5,7,8], and **Roberta Brambilla**[1,2,*]

[1]The Miami Project To Cure Paralysis, Department of Neurological Surgery, University of Miami Miller School of Medicine, Miami, FL 33136, USA

[2]Neuroscience Program, University of Miami Miller School of Medicine, Miami, FL 33136, USA

[3]Center for Computational Science, University of Miami Miller School of Medicine, Miami, FL 33136, USA

[4]Columbia University, New York, NY 10027, USA

[5]Department of Neurobiology Research, Institute of Molecular Medicine, University of Southern Denmark, Odense C, 5000, Denmark

[6]Department of Cellular and Molecular Pharmacology, University of Miami Miller School of Medicine, Miami, FL 33136, USA

[7]BRIDGE, Brain Research ◆ Inter-Disciplinary Guided Excellence, Department of Clinical Research, University of Southern Denmark, Odense C, 5000, Denmark

[8]Department of Neurology, Odense University Hospital, Odense C, 5000, Denmark

Summary

In multiple sclerosis (MS), soluble tumor necrosis factor (TNF) is detrimental via activation of TNF receptor 1 (TNFR1), whereas transmembrane TNF is beneficial primarily by activating TNF receptor 2 (TNFR2). Here we investigate the role of TNFR2 in microglia and monocytes/macrophages in experimental autoimmune encephalomyelitis (EAE), a model of MS, by cell-specific gene targeting. We show that TNFR2 ablation in microglia leads to early onset of EAE with increased leukocyte infiltration, T cell activation, and demyelination in the central nervous

*Corresponding author and lead contact: Roberta Brambilla, Ph.D., r.brambilla@miami.edu, tel: 305-243-3567, fax: 305-243-3914.

Author contributions

HG conducted experiments, analyzed data and drafted the manuscript; MD, JLB and VPL analyzed the RNA-seq data; CC did stereological counting; MT did western blotting and colony management; CDH did microglia cultures and colony management; DGE and KLL analyzed data; PMM conducted behavioral tests; RB conceived the study, conducted experiments, analyzed data and wrote the manuscript. All co-authors reviewed and edited the manuscript.

Accession numbers

The accession number for the sequencing data reported in this paper is GEO: GSE78082.

system (CNS). Conversely, TNFR2 ablation in monocytes/macrophages results in EAE suppression with impaired peripheral T cell activation, and reduced CNS T cell infiltration and demyelination. Our work uncovers a dichotomy of function for TNFR2 in myeloid cells, with microglial TNFR2 providing protective signals to contain disease, and monocyte/macrophagic TNFR2 driving immune activation and EAE initiation. This must be taken into account when targeting TNFR2 for therapeutic purposes in neuroinflammatory diseases.

Graphical Abstract

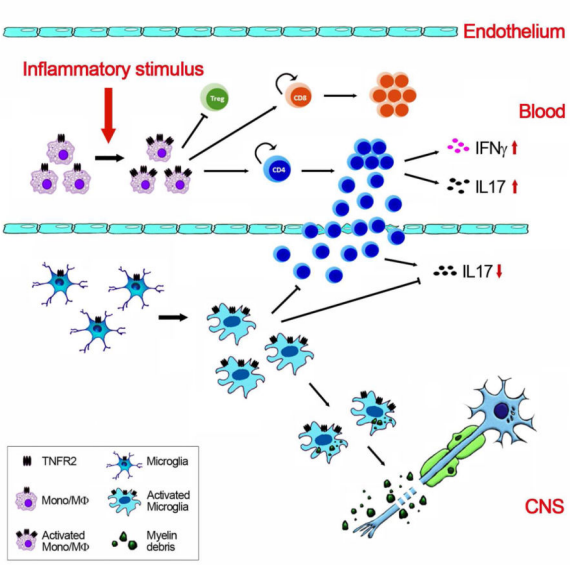

Introduction

Tumor necrosis factor (TNF) has been associated with the pathophysiology of multiple sclerosis (MS), as MS patients have high TNF concentrations in active lesions and cerebrospinal fluid, which correlate with the degree of disability (Hofman et al., 1989; Sharief and Hentges, 1991). TNF exists in two forms, transmembrane (tmTNF) and soluble (solTNF). solTNF derives from cleavage of tmTNF by the TNF-alpha converting enzyme (TACE). tmTNF signals via TNF receptor 1 (TNFR1; *Tnfrsf1a*) and TNF receptor 2 (TNFR2; *Tnfrsf1b*) although with higher affinity for TNFR2, while solTNF signals via TNFR1 (Grell et al., 1995; Wajant et al., 2003). TNFR1 is widely expressed and mediates the majority of solTNF-dependent effects in inflammation, apoptosis and neurotoxicity (Probert, 2015). Expression of TNFR2 is mostly restricted to immune and endothelial cells, where it sustains T^{reg} function (Chen and Oppenheim, 2010), suppresses Th17 differentiation (Miller et al., 2015), promotes lymphocyte proliferation (Tartaglia et al., 1993) and monocyte recruitment by endothelial cells (Venkatesh et al., 2013). In the central nervous system (CNS) TNFR2 is minimally expressed physiologically but is upregulated in microglia, astrocytes and oligodendrocytes in neurological disease (Brambilla et al., 2011; Lambertsen et al., 2007). TNFR2 is virtually absent in CNS neurons both in normal and pathological conditions (Brambilla et al., 2011; Probert, 2015), with motor neurons in a rodent model of ALS (Veglianese et al., 2006) and few neuron subsets in the Alzheimer's

brain (Cheng et al., 2010) being the only exceptions reported. TNFR2 has been suggested to play a role in neuroprotection and remyelination (Arnett et al., 2001; Fontaine et al., 2002; Marchetti et al., 2004; Patel et al., 2012), but little is known about its function in individual CNS cell lineages in vivo. Recent studies from our lab have addressed this void by cell-specific gene targeting approaches, demonstrating that oligodendroglial TNFR2 promotes oligodendrocyte differentiation and remyelination in experimental autoimmune encephalomyelitis (EAE), a model of MS (Madsen PM, 2016). Microglia and monocytes/macrophages (Mo/MΦ) play critical roles in MS and EAE (Shemer and Jung, 2015), and both express TNFR2 (Brambilla et al., 2011). However, the current knowledge of TNFR2 function in these populations is limited to only two in vitro studies: in microglia, TNFR2 was shown to promote the expression of antiinflammatory and neuroprotective genes (Veroni et al., 2010), and in macrophages to play an auxiliary role in activating proinflammatory TNFR1 signaling (Ruspi et al., 2014). Since TNFR2 function in microglia and Mo/MΦ in neurological disease is completely unknown, the goal of our study was to systematically dissect the roles TNFR2 in these populations in EAE etiopathology. Using conditional knockout (cKO) models we demonstrated that microglial TNFR2 is protective in the early stages of EAE, while monocyte/macrophagic TNFR2 is detrimental and drives disease initiation. Ablation of microglial TNFR2 accelerated EAE onset by establishing a proinflammatory environment that increased T cell activation in the CNS. In contrast, ablation of monocyte/macrophagic TNFR2 impaired T cell activation in the periphery resulting in reduced CNS immune cell infiltration and EAE suppression. Taken together, our data demonstrate the opposite functions of TNFR2 signaling in microglia and peripheral Mo/MΦ in the pathophysiology of EAE. This dichotomy needs to be addressed when targeting TNFR2 signaling for therapeutic purposes in MS or any other neuroinflammatory disease in which both cell populations are major contributors.

Results

Ablation of microglial TNFR2 in *Cx3cr1*^{CreER}:*Tnfrsf1b*$^{fl/fl}$ mice leads to the early onset of EAE

Selective gene targeting in microglia has been challenging due to their shared gene profile with Mo/MΦ. To restrict *Tnfrsf1b*$^{fl/fl}$ ablation to microglia we generated *Cx3cr1*^{CreER}:*Tnfrsf1b*$^{fl/fl}$ cKO mice and adopted an established tamoxifen (tam) induction protocol that exploits the different origins and turnover rates of microglia versus other $CX_3CR_1^+$ myeloid cells (Goldmann et al., 2013; Parkhurst et al., 2013). In this protocol, five daily tam injections are followed by a 28 day waiting period (instead of the usual 5–7 days) during which fast-renewing Mo/MΦ are replaced by wild type (WT) cells derived from bone marrow precursors, while self-renewing microglia are not replaced and maintain *Tnfrsf1b*$^{fl/fl}$ ablation. Even though specific microglial gene targeting has already been demonstrated with this protocol (Goldmann et al., 2013; Parkhurst et al., 2013), we still validated it in our own setting by comparison to a conventional 5-day waiting period. To do so, we crossed *Cx3cr1*^{CreER} mice, which constitutively express EYFP in $CX_3CR_1^+$ cells, with *Rosa26*$^{tdTomato+/-}$ reporters. In the spinal cord we detected recombination by tdTomato fluorescence in almost 90% of EYFP$^+$ microglia (Fig. S1A, S1C). In the spleen recombination was decreased from 40% to about 3% in EYFP$^+$ myeloid cells 28 days after

tam injection, confirming that gene targeting was restricted to $CX_3CR_1^+$ microglia and not Mo/MΦ (Fig. S1B, S1C). TNFR2 was barely present in microglia in naïve conditions (less than 5%, Fig. S2A–S2C) but was robustly upregulated after EAE (Fig. S2D–S2J) to about 70% in *Tnfrsf1b*$^{fl/fl}$ mice and was reduced to 30% in *Cx3cr1*^{CreER}:*Tnfrsf1b*$^{fl/fl}$ (Fig. S2D, S2E). Both splenic and CNS infiltrated Mo/MΦ highly expressed TNFR2 after EAE (Fig. S2F–S2I) with no difference between genotypes. These data demonstrate that *Cx3cr1*^{CreER}:*Tnfrsf1b*$^{fl/fl}$ mice induced with the 28 days tam protocol are an excellent model for selective TNFR2 ablation in microglia. Analysis with rotarod and open field tests showed no abnormal locomotor phenotype (Fig. S3A–S3C) or altered spontaneous activity (Fig. S3D–S3H) in naïve *Cx3cr1*^{CreER}:*Tnfrsf1b*$^{fl/fl}$ mice. Furthermore, microglial number was comparable to controls (Fig. S3I), and so was the expression of microglia-associated genes, such as *Trem2* and *P2ry12* (Fig. S3J). Notably, microglial *Tnfrsf1b*, which is minimally expressed in naïve microglia (Fig. S2A), did not change between *Tnfrsf1b*$^{fl/fl}$ and *Cx3cr1*^{CreER}:*Tnfrsf1b*$^{fl/fl}$ mice, which explains the lack of phenotypical alterations in naïve animals.

Induced with EAE, *Cx3cr1*^{CreER}:*Tnfrsf1b*$^{fl/fl}$ mice displayed earlier disease onset, though the clinical course later overlapped that of *Tnfrsf1b*$^{fl/fl}$ controls (Fig. 1A; Table S1). At 17 dpi, when the highest difference in clinical scores was observed, *Cx3cr1*^{CreER}:*Tnfrsf1b*$^{fl/fl}$ mice showed more robust microglial activation. Indeed, $CD45^{low}CD11b^+$ total microglia (Fig. 1B–1D) and $MHCII^+$ activated microglia (Fig. 1B, 1E) were significantly increased. This was due to enhanced proliferation, as shown by the higher number of $Ki67^+$ microglia (Fig. 1F, 1G), and not to an effect on survival, since the numbers of PI^-Annexin V^+ early apoptotic and PI^+Annexin V^+ late apoptotic/necrotic microglia were comparable between genotypes (Fig. 1H, 1I). Analysis of immune cell infiltration into the spinal cord showed a marked increase in CD4 T cells and $MHCII^+$ activated Mo/MΦ in *Cx3cr1*^{CreER}:*Tnfrsf1b*$^{fl/fl}$ mice (Fig. 1J–1L), which correlated with the earlier disease symptoms. $Ly6G^+$ neutrophils, total and $MHCII^+$ Mo/MΦ (Fig. 1K) were significantly lower, likely due to faster mobilization into circulation. Notably, *Cx3cr1*^{CreER}:*Tnfrsf1b*$^{fl/fl}$ mice had higher frequency of total and $MHCII^+$ splenic B cells (Fig. 1M, 1N), which indicates increased antigen presentation capacity and could explain, at least in part, the increased expansion of CD4 T cells.

Ablation of microglial TNFR2 leads to exacerbated T cell effector function in the spinal cord after EAE

Since EAE symptoms are largely driven by activated T cells, we tested T effector function by measuring Th1 and Th17 cytokines after ex vivo restimulation. In the spinal cord, infiltrated CD4 cells from *Cx3cr1*^{CreER}:*Tnfrsf1b*$^{fl/fl}$ mice showed increased IL17 production (Fig. 2A, 2C), but no changes in IFNγ and TNF (Fig. 2A–2C). No differences were found in splenic CD4 and CD8 cells (Fig. 2D–2I). This suggests that TNFR2 ablated microglia establishes an environment prone to driving T cells towards Th17 differentiation in the CNS. Interestingly, prior to disease onset (12 dpi) *Cx3cr1*^{CreER}:*Tnfrsf1b*$^{fl/fl}$ mice showed reduced expression of the tight junction protein ZO-1 in the spinal cord (Fig. 2J). By binding to other tight junction elements like Claudin-5 and Occludin, which did not change in our model (Fig. 2J), ZO-1 plays a crucial role in blood-brain barrier (BBB) integrity (Bennett et al.,

2010) and its downregulation is indicative of increased BBB permeability, which could contribute to the increased immune cell infiltration in *Cx3cr1*^{CreER}:*Tnfrsf1b*$^{fl/fl}$ mice (Fig. 1L).

Ablation of microglial TNFR2 leads to increased demyelination at chronic EAE

Even though *Cx3cr1*^{CreER}:*Tnfrsf1b*$^{fl/fl}$ and *Tnfrsf1b*$^{fl/fl}$ mice showed overlapping clinical profiles at chronic EAE, analysis of the spinal cord at 40 dpi revealed increased white matter damage in *Cx3cr1*^{CreER}:*Tnfrsf1b*$^{fl/fl}$ mice (Fig. 3A, 3B). This was paralleled by higher loss of Olig2^{+}CC1^{+} oligodendrocytes (Fig. 3C) and increase in Olig2^{+}PDGFRα^{+} oligodendrocyte precursor cells (OPCs) (Fig. 3D). Increased OPC numbers could depend on increased proliferation/survival to repair myelin damage (Maier et al., 2013), or on impaired differentiation into mature oligodendrocytes, as TNFR2 has been shown to regulate this process (Madsen et al., 2016). Analysis of axonal pathology showed no difference in the number of intact (Fig. 3E, 3F) or degenerated axons (Fig. 3E, 3G). This may explain the similar clinical scores at chronic disease despite myelin damage being more severe in *Cx3cr1*^{CreER}:*Tnfrsf1b*$^{fl/fl}$ mice.

TNFR2 ablated microglia develop a proinflammatory phenotype with dysregulated expression of homeostatic and host defense genes after EAE

To dissect the mechanisms by which microglial TNFR2 regulates EAE pathogenesis, we analyzed the transcriptome of spinal cord microglia from *Tnfrsf1b*$^{fl/fl}$ and *Cx3cr1*^{CreER}:*Tnfrsf1b*$^{fl/fl}$ mice at 17 dpi using RNA-seq (GEO: GSE78082). We found 5049 differentially expressed genes with high reproducibility across samples (Fig. 4A); 20% were upregulated (1022 genes) and 80% downregulated (4027 genes) in *Cx3cr1*^{CreER}:*Tnfrsf1b*$^{fl/fl}$ compared to *Tnfrsf1b*$^{fl/fl}$ mice (Fig. 4A), including *Tnfrsf1b* (Fig. 4C). Interestingly, *Tnfrsf1a* did not change (Fig. 4C, Fig. S4A), indicating that microglial TNFR2 does not have a modulatory function on TNFR1 at the transcriptional level. Changes were validated by qPCR on select genes and matched the RNA-seq data (Fig. S4A). Most of the downregulated genes belonged to pathways controlling cell homeostasis, such as MAPK and NF-κB (Fig. 4B), and were found to be physically or functionally connected with TNFR2 (Fig. S4B). Notably, the dysregulated genes included modulators of two key aspects of microglia innate immune function: inflammation, and host defense. With respect to inflammation, TNFR2 ablated microglia showed upregulation of chemokines (Fig. 4D), cell adhesion molecules, oxidative enzymes and growth factors (Fig. 4E), and downregulation of antiinflammatory signals like *Zfp36* and *Socs3* (Fig. 4F). With respect to host defense, microglia from *Cx3cr1*^{CreER}:*Tnfrsf1b*$^{fl/fl}$ mice showed dysregulation of the “microglial sensome” (Hickman et al., 2013), a set of molecules that define the microglial surveillance machinery. Only 7.1% of sensome genes were upregulated in *Cx3cr1*^{CreER}:*Tnfrsf1b*$^{fl/fl}$ mice, and over 46% downregulated (Fig. 4G). These include receptors for pathogen recognition (*Fcγr3*), phagocytosis (*Trem2*) (Fig. 4H), and tissue surveillance (Purinergic and Siglec receptors, Fig. 4I, 4J), suggesting that without TNFR2 key homeostatic functions of microglia may be altered. Phagocytosis was indeed compromised, as cultured microglia from *Tnfrsf1b*$^{-/-}$ mice showed a reduced capacity to engulf fluorescent beads both in unstimulated and LPS-stimulated conditions (Fig. 4K, 4L). Importantly, *Trem2* and *P2ry12* were reduced in *Tnfrsf1b*$^{-/-}$ unstimulated microglia (Fig. 4M, 4N), and further

downregulated in both genotypes after LPS stimulation. This suggests that TNFR2 activation is necessary for constitutive expression of these genes. *Trem2* and *P2ry12* were also assessed after stimulation with solTNF, which activates proinflammatory TNFR1. Unlike LPS, solTNF did not maintain suppression of *Trem2* and *P2ry12* in *Tnfrsf1b*−/− microglia (Fig. S4C). This indicates that transcriptional regulation of *Trem2* and *P2ry12* by solTNF depends not only on direct TNFR1 activation but also on the auxiliary presence of TNFR2. The cooperative signaling of TNFR1 and TNFR2 in myeloid cells has been also suggested in previous reports (Ruspi et al., 2014).

Collectively, these data indicate that without TNFR2 microglia develop a more invasive proinflammatory phenotype that accelerates EAE pathogenesis, while losing signals necessary to carry out essential homeostatic functions, including tissue surveillance and host defense.

Ablation of TNFR2 in *LysM*^{Cre}:*Tnfrsf1b*$^{fl/fl}$ mice results in suppression of EAE

To assess TNFR2 function in Mo/MΦ we used *LysM*^{Cre}:*Tnfrsf1b*$^{fl/fl}$ cKOs in combination with a bone marrow transplantation strategy. To start, we tested *LysM*^{Cre} recombination efficiency in peripheral and CNS myeloid cells by crossing *LysM*$^{Cre+/-}$ mice with *Rosa26*$^{tdTomato+/-}$ reporters. In splenic myeloid cells, recombination was similar in naïve and EAE conditions reaching approximately 50% (Fig. S5A, S5C). In spinal cord microglia, recombination was inefficient in naïve conditions with only 10% of $CD11b^{+}CX_3CR_1^{+}$ cells positive for tdTomato, which increased to 30% after EAE (Fig. S5B, S5D). TNFR2 expression, virtually absent in naïve conditions (Fig. S2A, S2B), amounted to over 60% of splenic Mo/MΦ and microglia in *Tnfrsf1b*$^{fl/fl}$ mice after EAE, and was significantly reduced in both populations in *LysM*^{Cre}:*Tnfrsf1b*$^{fl/fl}$ mice (Fig. S5E, S5F, S5I, S5J, Table S2). This was confirmed by immunohistochemistry (Fig. S5K). We also confirmed that TNFR2 ablation did not interfere with TNFR1 expression in splenic Mo/MΦ (Fig. S5G, S5H). Since the *LysM* promoter is active in granulocytes and other immune cells (Goldmann et al., 2013), to assess specificity of myeloid ablation we measured TNFR2 expression in various splenic populations (Table S2). TNFR2 was present in T cells, B cells and neutrophils with no difference between *Tnfrsf1b*$^{fl/fl}$ and *LysM*^{Cre}:*Tnfrsf1b*$^{fl/fl}$ mice. In NKs, TNFR2 was upregulated after EAE, with mild but significant reduction in *LysM*^{Cre}:*Tnfrsf1b*$^{fl/fl}$ mice. This should not influence the *LysM*^{Cre}:*Tnfrsf1b*$^{fl/fl}$ phenotype as NKs represent only a small fraction of the splenic population (less than 3%, Fig. 5E). It is worth noting that neuronal expression of Cre recombinase in *LysM*^{Cre} mice has been reported by various groups including ours (Clausen et al., 2016; Orthgiess et al., 2016). However, since TNFR2 is virtually absent in CNS neurons (Brambilla et al., 2011; Zhang et al., 2014), neuronal Cre activity should not affect TNFR2 expression in *LysM*^{Cre}:*Tnfrsf1b*$^{fl/fl}$ mice. Like *Cx3cr1*^{CreER}:*Tnfrsf1b*$^{fl/fl}$ mice, *LysM*^{Cre}:*Tnfrsf1b*$^{fl/fl}$ mice did not show alterations in locomotor function, spontaneous activity, or splenic leukocyte profile (Fig. S6).

To test myeloid TNFR2 function we induced EAE in *Tnfrsf1b*$^{fl/fl}$ and *LysM*^{Cre}:*Tnfrsf1b*$^{fl/fl}$ mice. Contrary to *Cx3Cr1*^{CreER}:*Tnfrsf1b*$^{fl/fl}$ cKOs, EAE was markedly suppressed in *LysM*^{Cre}:*Tnfrsf1b*$^{fl/fl}$ mice, with average scores below 2 (flaccid tail but no paralysis) (Fig. 5A, Table S3). Since TNFR2 ablation occurs in both Mo/MΦ and microglia in this model, to

dissect the contribution of each population to EAE development we generated bone marrow chimeras with gene ablation specific to either Mo/MΦ (*LysM*^{Cre}:*Tnfrsf1b*$^{fl/fl}$→CD45.1) or microglia (CD45.1→*LysM*^{Cre}:*Tnfrsf1b*$^{fl/fl}$). In *LysM*^{Cre}:*Tnfrsf1b*$^{fl/fl}$→CD45.1 mice EAE development and progression were suppressed (Fig. 5B), mirroring the profile of *LysM*^{Cre}:*Tnfrsf1b*$^{fl/fl}$ mice (Fig. 5A). Conversely, in CD45.1→*LysM*^{Cre}:*Tnfrsf1b*$^{fl/fl}$ mice EAE had accelerated onset and more severe progression (Fig. 5C), similarly to *Cx3cr1*^{CreER}:*Tnfrsf1b*$^{fl/fl}$ mice (Fig. 1A). At acute disease (20 dpi), the percentages of splenic cell populations in *LysM*^{Cre}:*Tnfrsf1b*$^{fl/fl}$ mice were comparable to *Tnfrsf1b*$^{fl/fl}$ mice (Fig. 5E), but the numbers of CD4 and CD8 T cells, B cells and MHCII^{+} activated B cells were reduced (Fig. 5G). The percentages of CNS infiltrated cells were also unchanged (Fig. 5D), but the absolute number of CD4 T cells was markedly lower (Fig. 5F). In addition, the microglial response was assessed, and though we did not see changes in cell number, we detected a reduction in the frequency of MHCII^{+} activated microglia in *LysM*^{Cre}:*Tnfrsf1b*$^{fl/fl}$ mice (Fig. 5H–5K), which could be a consequence of the reduced presence of proinflammatory CD4 cells in the spinal cord. These results indicate that TNFR2 ablation in Mo/MΦ and not microglia accounts for EAE suppression in *LysM*^{Cre}:*Tnfrsf1b*$^{fl/fl}$ mice, suggesting that TNFR2 in peripheral myeloid cells is required for EAE induction.

Ablation of TNFR2 in *LysM*^{Cre}:*Tnfrsf1b*$^{fl/fl}$ mice results in impaired T cell proliferation and effector function in the spleen after EAE

T cell expansion and activation are key for EAE initiation (Sospedra and Martin, 2005). Since we found reduced splenic T and B cells, and reduced infiltrated CD4 T cells in *LysM*^{Cre}:*Tnfrsf1b*$^{fl/fl}$ mice (Fig. 5F, 5G), we investigated whether TNFR2 ablation from Mo/MΦ impaired lymphocyte proliferation and activation preventing EAE induction. In the spleen, we analyzed proliferation at pre-disease (12 dpi) by Ki67 labeling and found in *LysM*^{Cre}:*Tnfrsf1b*$^{fl/fl}$ mice a reduction in Ki67^{+} CD4 and CD8 T cells, but no difference in B cells (Fig. 6A–6C). Effector function was assessed at acute disease (20 dpi) by measuring Th1 and Th17 cytokines. In splenic CD4 T cells TNF production did not change (Fig. S7A), but IFNγ and IL17 were reduced in *LysM*^{Cre}:*Tnfrsf1b*$^{fl/fl}$ mice (Fig. 6D, 6E). No differences were found in the CD8 population (Fig. S7B, S7C). On the contrary, IL17 was increased in infiltrated CD4 cells of *LysM*^{Cre}:*Tnfrsf1b*$^{fl/fl}$ mice (Fig. 6D, 6G), with no difference in CD8 cells (Fig. 6H, S7E). IFNγ and TNF did not change (Fig. S7D–S7F). Interestingly, *Cx3cr1*^{CreER}:*Tnfrsf1b*$^{fl/fl}$ mice showed a similar profile (Fig. 2A), suggesting that even minimal ablation of microglial TNFR2 as in *LysM*^{Cre}:*Tnfrsf1b*$^{fl/fl}$ mice may be sufficient to alter the CNS environment and promote Th17 differentiation.

We went further to test whether reduced T cell expansion and activation in *LysM*^{Cre}:*Tnfrsf1b*$^{fl/fl}$ mice could be associated with increased presence of regulatory cells in the spleen. We did not detect any changes in IL10 producing B1a and B1b B^{regs} (Fig. S7G, S7H), but we observed an increase in the frequency of CD25^{+}FoxP3^{+} T^{regs}. (Fig. 6I, 6J), which could contribute to the suppressed T cell response.

Together these data indicate that ablation of TNFR2 in peripheral Mo/MΦ compromises T cell activation and function resulting in inability to mount an efficient immune response and initiate EAE.

Ablation of TNFR2 in *LysM*^{Cre}:*Tnfrsf1b*$^{fl/fl}$ mice results in myelin preservation and neuroprotection in EAE

To investigate whether the improved functional outcome in *LysM*^{Cre}:*Tnfrsf1b*$^{fl/fl}$ mice corresponded to reduced myelin and axon pathology, we assessed white matter damage in the spinal cord by luxol fast blue staining. At 50 dpi *LysM*^{Cre}:*Tnfrsf1b*$^{fl/fl}$ mice showed reduced demyelination (Fig. 7A and 6B), accompanied by a higher number of Olig2^{+}PDGFRα^{+}OPCs (Fig. 7C). EM analysis of remyelination showed *LysM*^{Cre}:*Tnfrsf1b*$^{fl/fl}$ mice to have a higher number of remyelinated axons in the spinal cord (Fig. 7D and 7E) which, together with the higher presence of OPCs, suggests that repair mechanisms are more efficient in these mice. Evaluation of axonal damage showed significant neuroprotection in *LysM*^{Cre}:*Tnfrsf1b*$^{fl/fl}$ mice, with more intact axons (Fig. 7F and 7G) and reduced accumulation of degenerated axons (Fig. 7F and 7H), which correlated with the lower clinical scores at chronic EAE.

Discussion

In the present study we uncover a dichotomy of functions for microglial versus monocyte/macrophagic TNFR2 in EAE pathophysiology. We demonstrate that TNFR2 in microglia is protective by providing signals to contain neuroinflammation, while TNFR2 in Mo/MΦ is detrimental by driving immune activation and EAE initiation.

Microglia and monocytes are the main effectors of the innate immune response and, as such, perform homeostatic and surveillance functions sharing similar roles in different compartments, the CNS or the periphery (Ginhoux and Jung, 2014; Prinz et al., 2014). This explains why much of the molecular machinery is common to the two populations, despite their distinct developmental origin (Ginhoux et al., 2010). Exceptions to this rule are signature genes that have been recently identified as primarily expressed in one or the other, such as *P2ry12* and *Cx3cr1* found almost exclusively in microglia, and *P2rx4*, *Ccr2*, and *Ifitm* genes found uniquely in Mo/MΦ (Hickman et al., 2013). Capitalizing on this genetic diversity and developmental origin, the *Cx3Cr1*$^{CreER+/-}$ mouse line has allowed to specifically target microglia when using a tamoxifen induction protocol devised to take advantage of the different turnover rates of myeloid cells (Goldmann et al., 2013; Parkhurst et al., 2013; Yona et al., 2013). With this strategy we generated *Cx3cr1*^{CreER}:*Tnfrsf1b*$^{fl/fl}$ mice to dissect the role of microglial TNFR2 in EAE. Comparative transcriptome analysis shows that microglia are the neural cells with the highest expression of TNFR2 (http://web.stanford.edu/group/barres_lab/cgibin/igv_cgi_2.py?lname=Tnfrsf1b) (Zhang et al., 2014). Since tmTNF, the activating ligand of TNFR2, is protective in EAE (Brambilla et al., 2011; Taoufik et al., 2011), and in vitro evidence showed that TNFR2 is able to activate antiinflammatory signals (Veroni et al., 2010), we hypothesized that microglial TNFR2 could be the executor, at least in part, of tmTNF beneficial functions in vivo. In support of this hypothesis, *Cx3cr1*^{CreER}:*Tnfrsf1b*$^{fl/fl}$ mice developed EAE earlier, showing signs of paralysis more than two days in advance of *Tnfrsf1b*$^{fl/fl}$ controls. This was accompanied by elevated numbers and cellular activation of microglia at disease onset, paralleled by a higher CNS influx of activated immune cells. This indicates that TNFR2-dependent signals in microglia suppress neuroinflammation, and without them the CNS is more vulnerable to

immune-inflammatory attack from the periphery. As EAE progresses, the clinical profiles of the two genotypes converge and this may be due to more immune cells flooding the CNS and overcoming the antiinflammatory "barrier" set by microglial TNFR2. Nevertheless, our data underscore the protective role of microglial TNFR2 in the early stage of disease, which seems to participate in the immediate response of the CNS to alterations of its homeostasis.

To gain insight into the mechanisms of microglial TNFR2-dependent regulation of EAE, we performed RNA-seq analysis of the microglial transcriptome of *Cx3cr1*^{CreER}:*Tnfrsf1b*$^{fl/fl}$ and *Tnfrsf1b*$^{fl/fl}$ mice at disease onset. The picture that emerged is twofold. First, TNFR2 is crucial for microglial homeostatic functions. For example, TNFR2 ablation causes downregulation of the microglia-specific gene *Trem2*, which is necessary for innate immunity, phagocytosis and resolution of inflammation (Neumann and Takahashi, 2007). Loss-of-function mutations of *Trem2* in humans lead to neurodegenerative disease, including a form of late onset Alzheimer's disease (Guerreiro et al., 2013; Jonsson et al., 2013) where *Trem2* mutation has been suggested to disrupt microglial interaction with damaged neurons preventing their phagocytosis (Walter, 2016). Our in vitro data suggest that Trem2-dependent phagocytosis may be regulated by TNFR2. Indeed, without TNFR2 phagocytosis is drastically impaired, as is the expression of *Trem2*. The impaired ability of TNFR2 deficient microglia to respond to danger signals is reflected in the altered expression of the sensome genes, especially those required for detection of endogenous signals. This includes P2 purinergic receptors, which respond to ATP released by degenerating cells (Rodrigues et al., 2015), and Siglecs that keep microglia in a silent homeostatic status (Linnartz-Gerlach et al., 2014). Together, these data indicate that TNFR2 is an important signal for host defense and proper microglial response to injury.

The second key finding of the RNA-seq analysis is that TNFR2-ablated microglia display a more invasive and proinflammatory phenotype. For instance, genes encoding cell adhesion molecules were upregulated in microglia lacking TNFR2. One example is *Vcam-1*. VCAM-1^{+} microglial cells have been identified at the edges of MS lesions in proximity of oligodendrocyte cell bodies where oligodendrocyte loss occurs, suggesting that this contact may be detrimental to their survival (Peterson et al., 2002). Integrins (*Itgα1, Itgα4*) were also upregulated, and since they are known to modulate microglial migration and activation during neuroinflammation (Milner and Campbell, 2002), this further supports the idea that lack of TNFR2 exacerbates the microglial proinflammatory phenotype. This is also indicated by the upregulation of proinflammatory genes, such as chemokines. The elevated chemokine production by TNFR2 deficient microglia can help explain the increased influx of immune cells in *Cx3cr1*^{CreER}:*Tnfrsf1b*$^{fl/fl}$ mice. This may also be driven by a concomitant increase in BBB permeability, which is suggested by the early downregulation of ZO-1 expression. ZO-1 is decreased as early as 12 days after EAE induction, indicating that BBB alterations dependent on dysregulated TNFR2-ablated microglia could indeed be one of the earliest, and perhaps most critical, drivers of the exacerbated pathology in *Cx3cr1*^{CreER}:*Tnfrsf1b*$^{fl/fl}$ mice. In addition, the upregulation of *Vegfa* found in the RNA-seq screening also supports the idea of a more permeable BBB. Indeed, several reports have shown that CNS-derived VEGFA is implicated in BBB disruption, as its ablation prevents BBB breakdown and lymphocyte influx in EAE (Argaw et al., 2012; Argaw et al., 2009). Another interesting finding from the RNA-seq analysis is the upregulation of *Hgf* in

microglia of *Cx3cr1*^{CreER}:*Tnfrsf1b*$^{fl/fl}$ mice. HGF has been described as the primary microglial-derived chemotactic factor for OPCs, promoting their proliferation and migration to the site of demyelination (Lalive et al., 2005). This fits well with our data showing increased presence of OPCs in *Cx3cr1*^{CreER}:*Tnfrsf1b*$^{fl/fl}$ mice at chronic disease, where *Hgf* may serve as a reparative mechanism.

For a full understanding of myeloid TNFR2 function, the next step was to address the role of TNFR2 in peripheral Mo/MΦ, for which we used *LysM*^{Cre}:*Tnfrsf1b*$^{fl/fl}$ mice. As infiltrating monocytes and resident microglia both differentiate into macrophages which contribute to demyelination in EAE, the expectation was for monocyte/macrophagic TNFR2 to engage processes similar to those in microglia, resulting in worsening of the clinical outcome as in *Cx3cr1*^{CreER}:*Tnfrsf1b*$^{fl/fl}$ mice. Unexpectedly, our data showed the opposite, with *LysM*^{Cre}:*Tnfrsf1b*$^{fl/fl}$ mice being protected from EAE due to their inability to mount an efficient autoimmune response. This was dependent on impairment of two key steps in T cell activation: expansion and differentiation. Mo/MΦ can regulate these processes by presenting antigens and secreting cytokines (Hume, 2008; Wang et al., 2015) such as TGFβ1 and IL6. The concerted action of TGFβ1 and IL6 drives T cell expansion and also differentiation from naïve to a Th17 phenotype (Veldhoen et al., 2006), which is the key encephalitogenic population in EAE. Since both phenomena are suppressed in *LysM*^{Cre}:*Tnfrsf1b*$^{fl/fl}$ mice, it is possible that TNFR2 regulates the expression of these cytokines in Mo/MΦ. This idea is supported by our RNA-seq data where we saw a reduction of both TGFβ1 and IL6 signaling in TNFR2 deficient microglia. If this occurred also in Mo/MΦ, it would suggest that the opposite functions of microglial versus monocyte/macrophagic TNFR2 may depend not necessarily on the activation of distinct pathways, but on the engagement of the same pathways that lead to opposite effects due to the different compartments from where the cells originate.

TNFR2 in Mo/MΦ could also be regulating T cell expansion and differentiation indirectly by affecting regulatory T cells. T^{reg} frequency is increased in *LysM*^{Cre}:*Tnfrsf1b*$^{fl/fl}$ mice and their powerful suppressive activity may contribute to dampening T cell effector function in EAE. In addition to these mechanisms, we can't exclude the possibility that macrophagic TNFR2 may act via B cell modulation. Indeed we showed that *LysM*^{Cre}:*Tnfrsf1b*$^{fl/fl}$ mice have reduced MHCII expressing B cells in the spleen. Their compromised antigen presentation capacity could be in part responsible for the reduced EAE severity.

As far as tmTNF expressing cells that interact with microglia and Mo/MΦ to carry out TNFR2 functions, they may differ in physiological and pathological conditions. In the normal CNS, microglial TNFR2 will exert its beneficial homeostatic functions likely via contact with tmTNF-expressing microglia and astrocytes. In injury conditions, the repertoire of possible microglial TNFR2 activators widens as all CNS cells (including neurons), and infiltrating immune cells upregulate TNF production (Probert, 2015). Microglia, however, remain the most efficient TNF producers (Olmos and Llado, 2014), suggesting that much of the tmTNF-TNFR2 protective signaling may be driven by a microglial cell autonomous process both under physiological and pathological conditions. In the periphery, TNFR2-expressing Mo/MΦ may encounter their tmTNF ligand on virtually all leukocytes, particularly in disease conditions, but also on endothelial and stromal cells, such as

fibroblasts and pericytes. Among leukocytes, dendritic cells may be important partners of TNFR2-expressing Mo/MΦ, as they have been shown to play important roles in innate immune regulation precisely via tmTNF (Xu et al., 2007).

Overall, our study fits within the now accepted model that in pathological conditions the contribution of microglia and peripheral myeloid cells to disease etiology, progression and resolution may diverge (Shemer and Jung, 2015). In EAE, for example, Yamasaki and colleagues elegantly showed that peripherally derived macrophages associate with nodes of Ranvier and initiate demyelination, while microglia take on a protective function by clearing cellular debris (Yamasaki et al., 2014). In this context, we propose TNFR2 as one of the possible effectors of this dual behavior, as TNF production and TNFR2 expression are highly upregulated following EAE in myeloid cells.

Finally, our work further highlights the complexity of TNF function in neuroimmune disease. Not only does TNF have opposite roles whether in soluble or transmembrane form, with solTNF being proinflammatory and tmTNF protective, but so it does its receptor TNFR2 depending on the location in central or peripheral myeloid cells. This must be taken into account from a clinical perspective, as strategies enhancing TNFR2 signaling have been proposed as therapeutic avenues in neurodegenerative diseases (Dong et al., 2016; Maier et al., 2013). TNFR2 agonists specifically targeted to the CNS via ad hoc delivery systems at the appropriate time may be a viable pharmacological approach provided their effects on peripheral immune activation are minimized.

Experimental procedures

Mice

Adult (2–4 months) female and male mice were used in this study. Mice with conditional ablation of the TNFR2 gene (*Tnfrsf1b*) were generated by crossing *Cx3cr1*$^{\text{CreER;EYFP+/−}}$ (Jackson Lab, 021160) and *LysM*$^{\text{Cre+/−}}$ mice (Jackson Lab, 004781) with *Tnfrsf1b*$^{fl/fl}$ mice. *Tnfrsf1b*$^{fl/fl}$ mice were obtained by breeding C57BL/6NTac-Tnfrsf1b$^{\text{tm1a(EUCOMM)Wtsi/Ics}}$ mice (European Mouse Mutant Archive) with an FLP deleter (Jackson Lab, 009086) to remove the FRT-flanked neomycin cassette. In all experiments *Tnfrsf1b*$^{fl/fl}$ littermates were used as controls. In *Cx3cr1*$^{\text{CreER}}$:*Tnfrsf1b*$^{fl/fl}$ mice Cre recombinase was induced by 5 daily i.p. tam injections (2 mg/mouse/day) followed by a 28-days waiting period. Control mice received the same treatment. *Rosa26*$^{\text{tdTomato+/−}}$ reporter mice (007914) and CD45.1 congenic C57BL/6 mice (002014) were obtained from Jackson Laboratory. Colonies were housed in the virus/antigen-free Animal Core Facility of The Miami Project to Cure Paralysis, with a 12 h light/dark cycle, controlled temperature and humidity, and were provided with water and food ad libitum. Experiments were performed according to protocols approved by the Institutional Animal Care and Use Committee of the University of Miami.

Behavioral assessments

Open Field and Rotarod tests were performed as previously described (Madsen et al., 2015)

Induction of experimental autoimmune encephalomyelitis (EAE)

Active EAE was induced with $MOG_{35–55}$ peptide as previously described (Brambilla et al., 2014).

Isolation of leukocytes from spinal cord and spleen

Cells were isolated as previously described (Brambilla et al., 2014).

Bone marrow transplantation

Bone marrow transplantation was performed as previously described (Ashbaugh et al., 2013).

Luxol fast blue staining and quantification of demyelinated white matter volume

PFA-fixed segments of the spinal cord were paraffin-embedded, sectioned into 15 μm thick cross sections with a Leica RM 2135 microtome, and stained with luxol fast blue (LFB) and hematoxylin & eosin (H&E). Twenty serial sections at 120 μm intervals were used to estimate the demyelinated white matter volume. Demyelinated areas were outlined with an Olympus BX51 microscope, and demyelinated white matter volume quantified with Stereoinvestigator software (MicroBrightfield Inc.). 3D reconstructions of the demyelinated spinal cord were performed on the same serial sections with Neurolucida software (MBF Bioscience).

Toluidine blue staining and electron microscopy (EM) tissue preparation

These procedures were performed as previously described (Brambilla et al., 2014)

Statistical analysis

Statistical analysis of EAE clinical course was carried out with the Mann-Whitney U test. For analysis of RNA-seq data see Supplemental Experimental Procedures. All other data were analyzed by one-way ANOVA followed by Tukey test for multiple comparisons. In single comparisons, Student’s t test was applied. P values equal to or less than 0.05 were considered statistically significant. Data were expressed as the average of multiple determinations ± SEM. Statistical analyses were performed with Prism software.

For all other methods, protocols and materials see Supplemental Experimental Procedures.

Supplementary Material

Refer to Web version on PubMed Central for supplementary material.

Acknowledgments

We thank Drs. Jae Lee and Yunjiao Zhu for assistance with reporter mice and mouse chimera generation; Drs. Poincyane Assis-Nascimento and Dan Liebl for assistance with western blot of tight junction proteins; Margaret Bates and Vania Almeida for EM and toluidine blue staining; Dr. Melissa Carballosa-Gautam for advise in histological analyses; Dr. Oliver Umland for advise in flow cytometry experiments. The authors declare no competing financial interests. This work was supported by NINDS grants NS084303-01A1 and 1R01NS094522-01 (RB); FISM (Italian Multiple Sclerosis Foundation) grant 2012/R/2 (RB); The Miami Project To Cure Paralysis and the Buoniconti Fund (RB); Danish MS Society grant R431-A29647-B20593 (KLL).

References

Argaw AT, Asp L, Zhang J, Navrazhina K, Pham T, Mariani JN, Mahase S, Dutta DJ, Seto J, Kramer EG, et al. Astrocyte-derived VEGF-A drives blood-brain barrier disruption in CNS inflammatory disease. J Clin Invest. 2012; 122:2454–2468. [PubMed: 22653056]

Argaw AT, Gurfein BT, Zhang Y, Zameer A, John GR. VEGF-mediated disruption of endothelial CLN-5 promotes blood-brain barrier breakdown. Proc Natl Acad Sci U S A. 2009; 106:1977–1982. [PubMed: 19174516]

Arnett HA, Mason J, Marino M, Suzuki K, Matsushima GK, Ting JP. TNF alpha promotes proliferation of oligodendrocyte progenitors and remyelination. Nat Neurosci. 2001; 4:1116–1122. [PubMed: 11600888]

Bennett J, Basivireddy J, Kollar A, Biron KE, Reickmann P, Jefferies WA, McQuaid S. Blood-brain barrier disruption and enhanced vascular permeability in the multiple sclerosis model EAE. J Neuroimmunol. 2010; 229:180–191. [PubMed: 20832870]

Brambilla R, Ashbaugh JJ, Magliozzi R, Dellarole A, Karmally S, Szymkowski DE, Bethea JR. Inhibition of soluble tumour necrosis factor is therapeutic in experimental autoimmune encephalomyelitis and promotes axon preservation and remyelination. Brain. 2011; 134:2736–2754. [PubMed: 21908877]

Chen X, Oppenheim JJ. TNF-alpha: an activator of CD4+FoxP3+TNFR2+ regulatory T cells. Curr Dir Autoimmun. 2010; 11:119–134. [PubMed: 20173391]

Cheng X, Yang L, He P, Li R, Shen Y. Differential activation of tumor necrosis factor receptors distinguishes between brains from Alzheimer's disease and non-demented patients. J Alzheimers Dis. 2010; 19:621–630. [PubMed: 20110607]

Clausen BH, Degn M, Sivasaravanaparan M, Fogtmann T, Andersen MG, Trojanowsky MD, Gao H, Hvidsten S, Baun C, Deierborg T, et al. Conditional ablation of myeloid TNF increases lesion volume after experimental stroke in mice, possibly via altered ERK1/2 signaling. Sci Rep. 2016; 6:29291. [PubMed: 27384243]

Dong Y, Fischer R, Naude PJ, Maier O, Nyakas C, Duffey M, Van der Zee EA, Dekens D, Douwenga W, Herrmann A, et al. Essential protective role of tumor necrosis factor receptor 2 in neurodegeneration. Proc Natl Acad Sci U S A. 2016; 113:12304–12309. [PubMed: 27791020]

Fontaine V, Mohand-Said S, Hanoteau N, Fuchs C, Pfizenmaier K, Eisel U. Neurodegenerative and neuroprotective effects of tumor Necrosis factor (TNF) in retinal ischemia: opposite roles of TNF receptor 1 and TNF receptor 2. J Neurosci. 2002; 22:RC216. [PubMed: 11917000]

Ginhoux F, Greter M, Leboeuf M, Nandi S, See P, Gokhan S, Mehler MF, Conway SJ, Ng LG, Stanley ER, et al. Fate mapping analysis reveals that adult microglia derive from primitive macrophages. Science. 2010; 330:841–845. [PubMed: 20966214]

Ginhoux F, Jung S. Monocytes and macrophages: developmental pathways and tissue homeostasis. Nat Rev Immunol. 2014; 14:392–404. [PubMed: 24854589]

Goldmann T, Wieghofer P, Muller PF, Wolf Y, Varol D, Yona S, Brendecke SM, Kierdorf K, Staszewski O, Datta M, et al. A new type of microglia gene targeting shows TAK1 to be pivotal in CNS autoimmune inflammation. Nat Neurosci. 2013; 16:1618–1626. [PubMed: 24077561]

Grell M, Douni E, Wajant H, Lohden M, Clauss M, Maxeiner B, Georgopoulos S, Lesslauer W, Kollias G, Pfizenmaier K, et al. The transmembrane form of tumor necrosis factor is the prime activating ligand of the 80 kDa tumor necrosis factor receptor. Cell. 1995; 83:793–802. [PubMed: 8521496]

Guerreiro R, Wojtas A, Bras J, Carrasquillo M, Rogaeva E, Majounie E, Cruchaga C, Sassi C, Kauwe JS, Younkin S, et al. TREM2 variants in Alzheimer's disease. N Engl J Med. 2013; 368:117–127. [PubMed: 23150934]

Hickman SE, Kingery ND, Ohsumi TK, Borowsky ML, Wang LC, Means TK, El Khoury J. The microglial sensome revealed by direct RNA sequencing. Nat Neurosci. 2013; 16:1896–1905. [PubMed: 24162652]

Hofman FM, Hinton DR, Johnson K, Merrill JE. Tumor necrosis factor identified in multiple sclerosis brain. J Exp Med. 1989; 170:607–612. [PubMed: 2754393]

Hume DA. Macrophages as APC and the dendritic cell myth. J Immunol. 2008; 181:5829–5835. [PubMed: 18941170]

Jonsson T, Stefansson H, Steinberg S, Jonsdottir I, Jonsson PV, Snaedal J, Bjornsson S, Huttenlocher J, Levey AI, Lah JJ, et al. Variant of TREM2 associated with the risk of Alzheimer's disease. N Engl J Med. 2013; 368:107–116. [PubMed: 23150908]

Lalive PH, Paglinawan R, Biollaz G, Kappos EA, Leone DP, Malipiero U, Relvas JB, Moransard M, Suter T, Fontana A. TGF-beta-treated microglia induce oligodendrocyte precursor cell chemotaxis through the HGF-c-Met pathway. Eur J Immunol. 2005; 35:727–737. [PubMed: 15724248]

Lambertsen KL, Clausen BH, Fenger C, Wulf H, Owens T, Dagnaes-Hansen F, Meldgaard M, Finsen B. Microglia and macrophages express tumor necrosis factor receptor p75 following middle cerebral artery occlusion in mice. Neuroscience. 2007; 144:934–949. [PubMed: 17161916]

Linnartz-Gerlach B, Kopatz J, Neumann H. Siglec functions of microglia. Glycobiology. 2014; 24:794–799. [PubMed: 24833613]

Madsen PM MD, Karmally S, Szymkowski DE, Lambertsen KL, Bethea JR, Brambilla R. Oligodendroglial TNFR2 mediates membrane TNF-dependent repair in experimental autoimmune encephalomyelitis by promoting oligodendrocyte differentiation and remyelination. J Neurosci. 2016; 36:5128–5143. [PubMed: 27147664]

Madsen PM, Motti D, Karmally S, Szymkowski DE, Lambertsen KL, Bethea JR, Brambilla R. Oligodendroglial TNFR2 Mediates Membrane TNF-Dependent Repair in Experimental Autoimmune Encephalomyelitis by Promoting Oligodendrocyte Differentiation and Remyelination. J Neurosci. 2016; 36:5128–5143. [PubMed: 27147664]

Maier O, Fischer R, Agresti C, Pfizenmaier K. TNF receptor 2 protects oligodendrocyte progenitor cells against oxidative stress. Biochem Biophys Res Commun. 2013; 440:336–341. [PubMed: 24076392]

Marchetti L, Klein M, Schlett K, Pfizenmaier K, Eisel UL. Tumor necrosis factor (TNF)-mediated neuroprotection against glutamate-induced excitotoxicity is enhanced by N-methyl-D-aspartate receptor activation. Essential role of a TNF receptor 2-mediated phosphatidylinositol 3-kinase-dependent NF-kappa B pathway. J Biol Chem. 2004; 279:32869–32881. [PubMed: 15155767]

Miller PG, Bonn MB, McKarns SC. Transmembrane TNF-TNFR2 Impairs Th17 Differentiation by Promoting Il2 Expression. J Immunol. 2015; 195:2633–2647. [PubMed: 26268655]

Milner R, Campbell IL. The integrin family of cell adhesion molecules has multiple functions within the CNS. J Neurosci Res. 2002; 69:286–291. [PubMed: 12125070]

Neumann H, Takahashi K. Essential role of the microglial triggering receptor expressed on myeloid cells-2 (TREM2) for central nervous tissue immune homeostasis. J Neuroimmunol. 2007; 184:92–99. [PubMed: 17239445]

Olmos G, Llado J. Tumor necrosis factor alpha: a link between neuroinflammation and excitotoxicity. Mediators Inflamm. 2014; 2014:861231. [PubMed: 24966471]

Orthgiess J, Gericke M, Immig K, Schulz A, Hirrlinger J, Bechmann I, Eilers J. Neurons exhibit Lyz2 promoter activity in vivo: Implications for using LysM-Cre mice in myeloid cell research. Eur J Immunol. 2016

Parkhurst CN, Yang G, Ninan I, Savas JN, Yates JR 3rd, Lafaille JJ, Hempstead BL, Littman DR, Gan WB. Microglia promote learning-dependent synapse formation through brain-derived neurotrophic factor. Cell. 2013; 155:1596–1609. [PubMed: 24360280]

Patel JR, Williams JL, Muccigrosso MM, Liu L, Sun T, Rubin JB, Klein RS. Astrocyte TNFR2 is required for CXCL12-mediated regulation of oligodendrocyte progenitor proliferation and differentiation within the adult CNS. Acta Neuropathol. 2012; 124:847–860. [PubMed: 22933014]

Peterson JW, Bo L, Mork S, Chang A, Ransohoff RM, Trapp BD. VCAM-1-positive microglia target oligodendrocytes at the border of multiple sclerosis lesions. J Neuropathol Exp Neurol. 2002; 61:539–546. [PubMed: 12071637]

Prinz M, Tay TL, Wolf Y, Jung S. Microglia: unique and common features with other tissue macrophages. Acta Neuropathol. 2014; 128:319–331. [PubMed: 24652058]

Probert L. TNF and its receptors in the CNS: The essential, the desirable and the deleterious effects. Neuroscience. 2015

Rodrigues RJ, Tome AR, Cunha RA. ATP as a multi-target danger signal in the brain. Front Neurosci. 2015; 9:148. [PubMed: 25972780]

Ruspi G, Schmidt EM, McCann F, Feldmann M, Williams RO, Stoop AA, Dean JL. TNFR2 increases the sensitivity of ligand-induced activation of the p38 MAPK and NF-kappaB pathways and signals TRAF2 protein degradation in macrophages. Cell Signal. 2014; 26:683–690. [PubMed: 24378531]

Sharief MK, Hentges R. Association between tumor necrosis factor-alpha and disease progression in patients with multiple sclerosis. N Engl J Med. 1991; 325:467–472. [PubMed: 1852181]

Shemer A, Jung S. Differential roles of resident microglia and infiltrating monocytes in murine CNS autoimmunity. Semin Immunopathol. 2015

Sospedra M, Martin R. Immunology of multiple sclerosis. Annu Rev Immunol. 2005; 23:683–747. [PubMed: 15771584]

Taoufik E, Tseveleki V, Chu SY, Tselios T, Karin M, Lassmann H, Szymkowski DE, Probert L. Transmembrane tumour necrosis factor is neuroprotective and regulates experimental autoimmune encephalomyelitis via neuronal nuclear factor-kappaB. Brain. 2011; 134:2722–2735. [PubMed: 21908876]

Tartaglia LA, Goeddel DV, Reynolds C, Figari IS, Weber RF, Fendly BM, Palladino MA Jr. Stimulation of human T-cell proliferation by specific activation of the 75-kDa tumor necrosis factor receptor. J Immunol. 1993; 151:4637–4641. [PubMed: 8409424]

Veglianese P, Lo Coco D, Bao Cutrona M, Magnoni R, Pennacchini D, Pozzi B, Gowing G, Julien JP, Tortarolo M, Bendotti C. Activation of the p38MAPK cascade is associated with upregulation of TNF alpha receptors in the spinal motor neurons of mouse models of familial ALS. Mol Cell Neurosci. 2006; 31:218–231. [PubMed: 16219474]

Veldhoen M, Hocking RJ, Atkins CJ, Locksley RM, Stockinger B. TGFbeta in the context of an inflammatory cytokine milieu supports de novo differentiation of IL-17-producing T cells. Immunity. 2006; 24:179–189. [PubMed: 16473830]

Venkatesh D, Ernandez T, Rosetti F, Batal I, Cullere X, Luscinskas FW, Zhang Y, Stavrakis G, Garcia-Cardena G, Horwitz BH, et al. Endothelial TNF receptor 2 induces IRF1 transcription factor-dependent interferon-beta autocrine signaling to promote monocyte recruitment. Immunity. 2013; 38:1025–1037. [PubMed: 23623383]

Veroni C, Gabriele L, Canini I, Castiello L, Coccia E, Remoli ME, Columba-Cabezas S, Arico E, Aloisi F, Agresti C. Activation of TNF receptor 2 in microglia promotes induction of anti-inflammatory pathways. Mol Cell Neurosci. 2010; 45:234–244. [PubMed: 20600925]

Wajant H, Pfizenmaier K, Scheurich P. Tumor necrosis factor signaling. Cell Death Differ. 2003; 10:45–65. [PubMed: 12655295]

Walter J. The Triggering Receptor Expressed on Myeloid Cells 2: A Molecular Link of Neuroinflammation and Neurodegenerative Diseases. J Biol Chem. 2016; 291:4334–4341. [PubMed: 26694609]

Wang C, Collins M, Kuchroo VK. Effector T cell differentiation: are master regulators of effector T cells still the masters? Curr Opin Immunol. 2015; 37:6–10. [PubMed: 26319196]

Xu J, Chakrabarti AK, Tan JL, Ge L, Gambotto A, Vujanovic NL. Essential role of the TNF-TNFR2 cognate interaction in mouse dendritic cell-natural killer cell crosstalk. Blood. 2007; 109:3333–3341. [PubMed: 17164346]

Yamasaki R, Lu H, Butovsky O, Ohno N, Rietsch AM, Cialic R, Wu PM, Doykan CE, Lin J, Cotleur AC, et al. Differential roles of microglia and monocytes in the inflamed central nervous system. J Exp Med. 2014; 211:1533–1549. [PubMed: 25002752]

Yona S, Kim KW, Wolf Y, Mildner A, Varol D, Breker M, Strauss-Ayali D, Viukov S, Guilliams M, Misharin A, et al. Fate mapping reveals origins and dynamics of monocytes and tissue macrophages under homeostasis. Immunity. 2013; 38:79–91. [PubMed: 23273845]

Zhang Y, Chen K, Sloan SA, Bennett ML, Scholze AR, O'Keeffe S, Phatnani HP, Guarnieri P, Caneda C, Ruderisch N, et al. An RNA-sequencing transcriptome and splicing database of glia, neurons, and vascular cells of the cerebral cortex. J Neurosci. 2014; 34:11929–11947. [PubMed: 25186741]

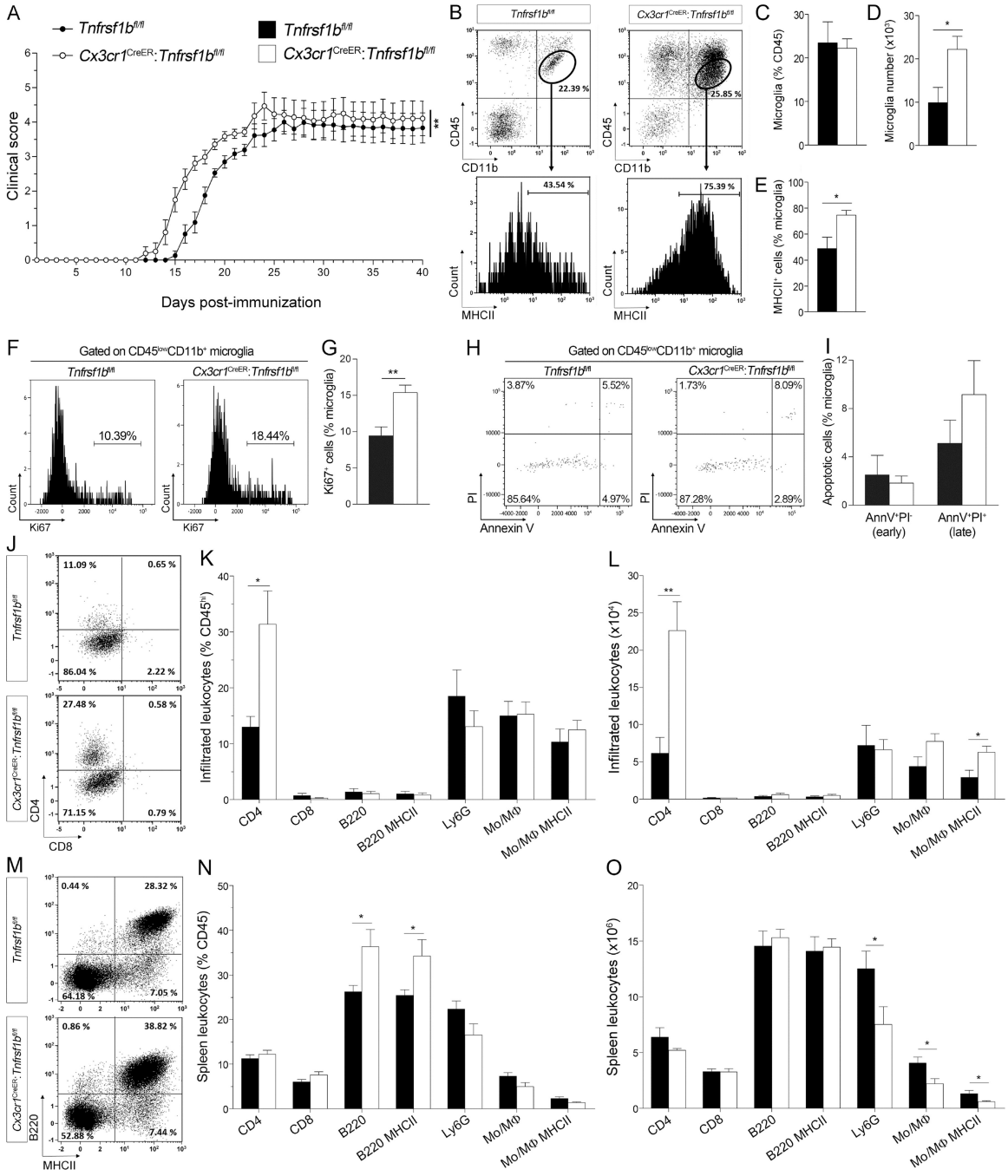

Figure 1. Ablation of microglial TNFR2 in *Cx3cr1*^{CreER}:*Tnfrsf1b*$^{fl/fl}$ mice leads to the early onset of EAE

A) Clinical course of EAE in *Tnfrsf1b*$^{fl/fl}$ and *Cx3cr1*^{CreER}:*Tnfrsf1b*$^{fl/fl}$ mice; n=13–17/group from two experiments; **p ≤ 0.01, one-way ANOVA, Mann-Whitney test. (B–E) Flow cytometric analysis of microglia in the spinal cord at 17 dpi EAE. (C, D) Quantification of percentage (C) and number (D) of microglia, and percentage of MHCII^{+} activated microglia (E); n=5/group, *p ≤ 0.05, Student's *t* test. (F) Representative flow plots of Ki67 expression in microglia at 17 dpi. (G) Quantification of Ki67^{+} microglia; n=4–5/group, *p ≤ 0.01, Student's *t* test. (H) Representative flow plots of Annexin V expression in

microglia at 17 dpi. (I) Quantification of Annexin V^+PI^- and Annexin V^+PI^- microglia; n=4–5/group. (J) Representative flow plots of CD4 and CD8 cells in the spinal cord at 17 dpi. (K, L) Percentages (K) and absolute numbers (L) of infiltrated immune cells. Mo/MΦ are defined as $CD45^{hi}CD11b^+NK1.1^-Ly6G^-SSA^{low}$; n=5/group, *p ≤ 0.05, **p ≤ 0.01, Student's *t* test. (M) Representative flow plots of total and $MHCII^+$ splenic B cells at 17 dpi. (N, O) Percentages (N) and absolute numbers (O) of splenic immune cells; n=6/group, *p ≤ 0.05, Student's *t* test.

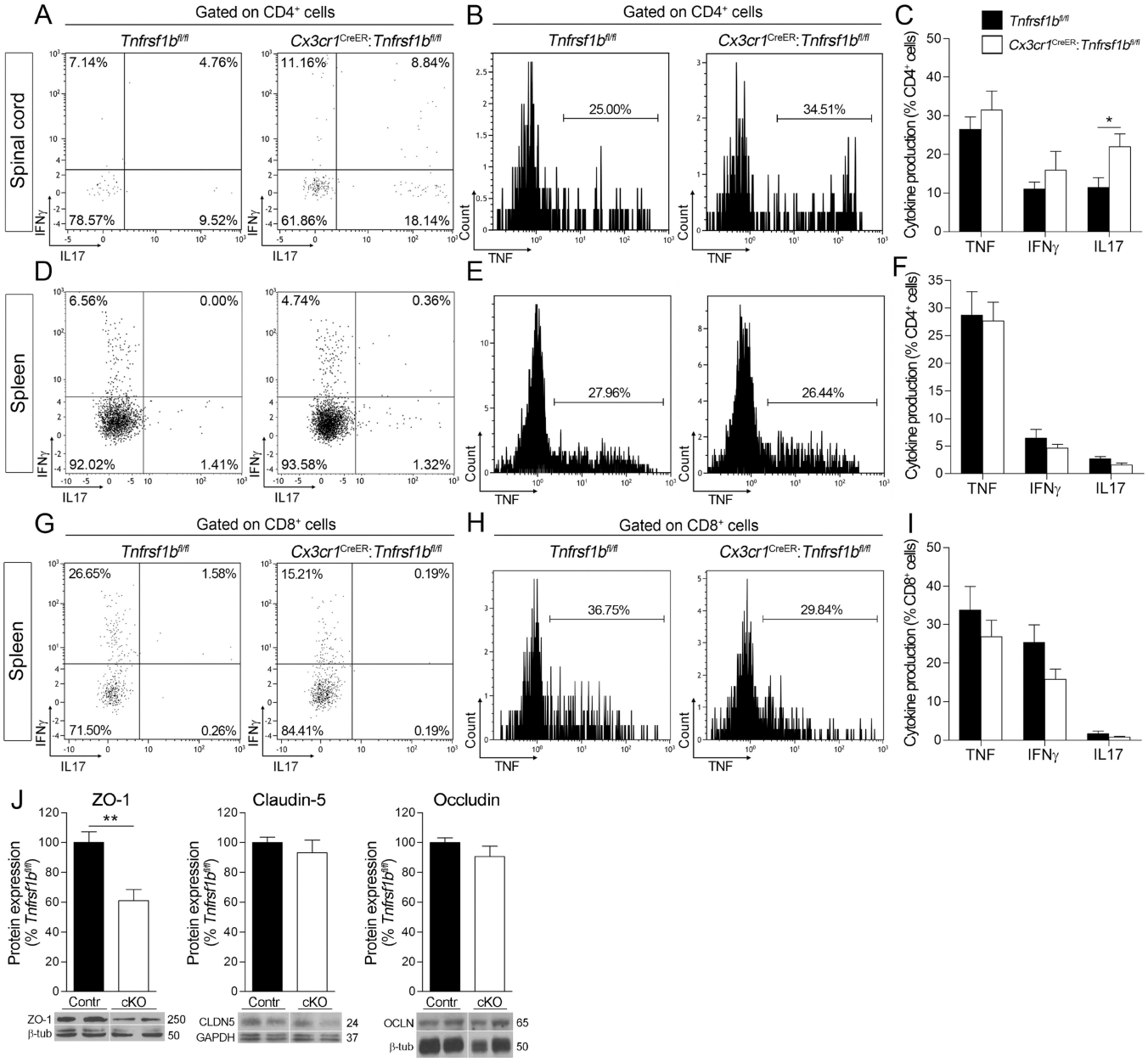

Figure 2. Ablation of microglial TNFR2 leads to exacerbated T cell effector function in the spinal cord after EAE

A, B, D, E, G, H) Representative flow plots of cytokine expression in CD4 and CD8 T cells isolated from spinal cord and spleen of *Tnfrsf1b*$^{fl/fl}$ and *Cx3cr1*^{CreER}:*Tnfrsf1b*$^{fl/fl}$ mice at 17 dpi; n=4–5/group, *p ≤ 0.05, Student's *t* test. (C, F, I) Quantification of cytokine expression in CD4 and CD8 T cells from spinal cord and spleen; n=4–5/group. (J) Western blot analysis of tight junction proteins in the spinal cord at 12 dpi EAE; n=4–9/group, **p ≤ 0.01, Student's *t* test.

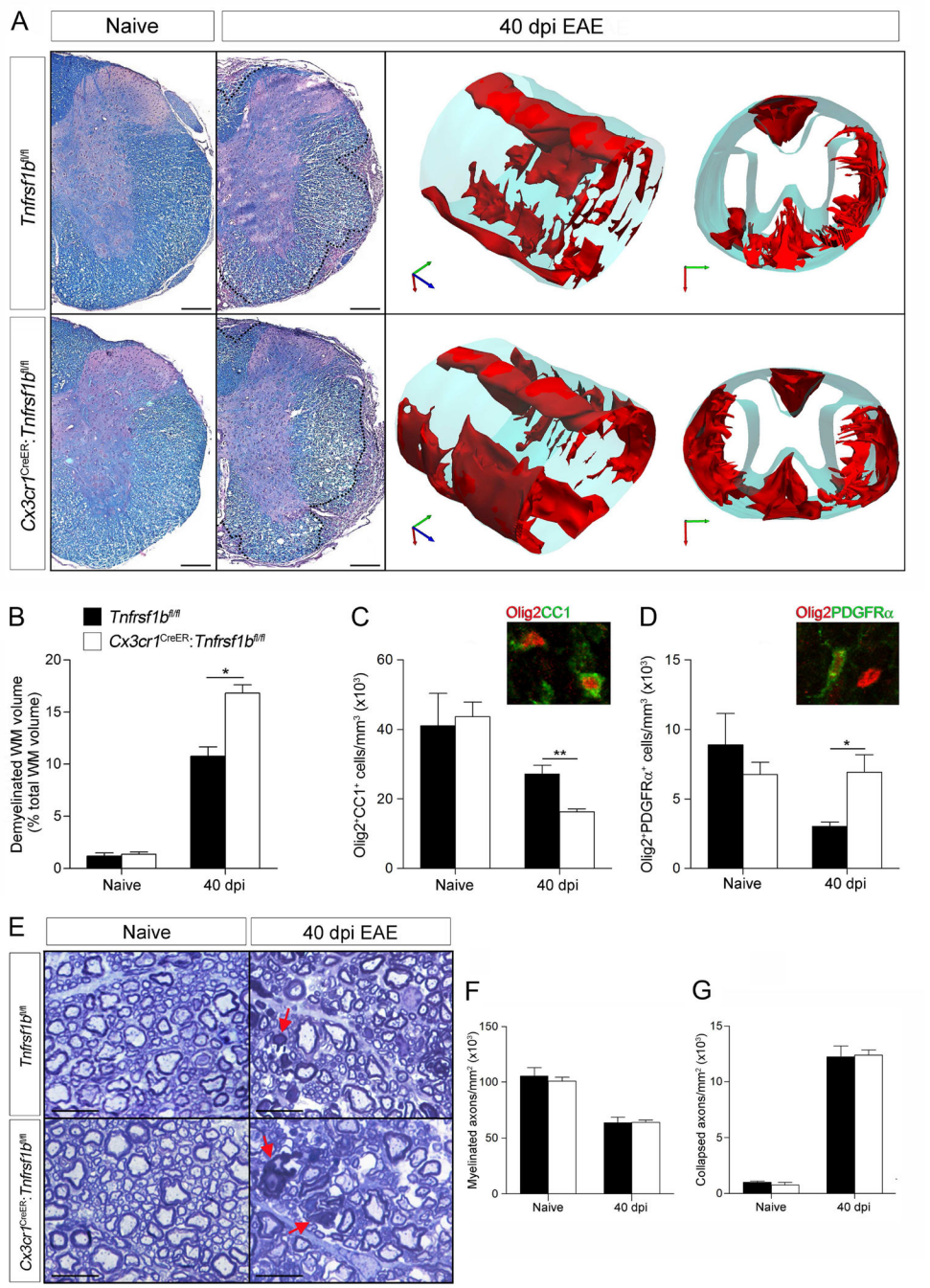

Figure 3. Microglial TNFR2 ablation leads to increased demyelination at chronic EAE

A) Assessment of demyelination in the spinal cord of *Tnfrsf1b*$^{fl/fl}$ and *Cx3cr1*^{CreER}:*Tnfrsf1b*$^{fl/fl}$ mice by LFB staining. Left: contoured areas show regions of demyelinated white matter; scale bar = 200 μm. Right: 3D reconstructions of the demyelinated areas (red). (B) Quantification of the demyelinated white matter volume; n=3–5/group, *p ≤ 0.05, Student's *t* test. (C, D) Quantification of Olig2^{+}CC1^{+} cells (C) and Olig2^{+}PDGFRα^{+} cells (D) in the spinal cord; n=3–5/group, *p ≤ 0.05, **p ≤ 0.01, Student's *t* test. (E) Toluidine blue staining of spinal cord sections from naive and 40 dpi mice. Red

arrows indicate degenerated collapsed axons; scale bar =10 μm. (F, G) Quantification of myelinated (F) and degenerated (G) axons; n=4–5/group.

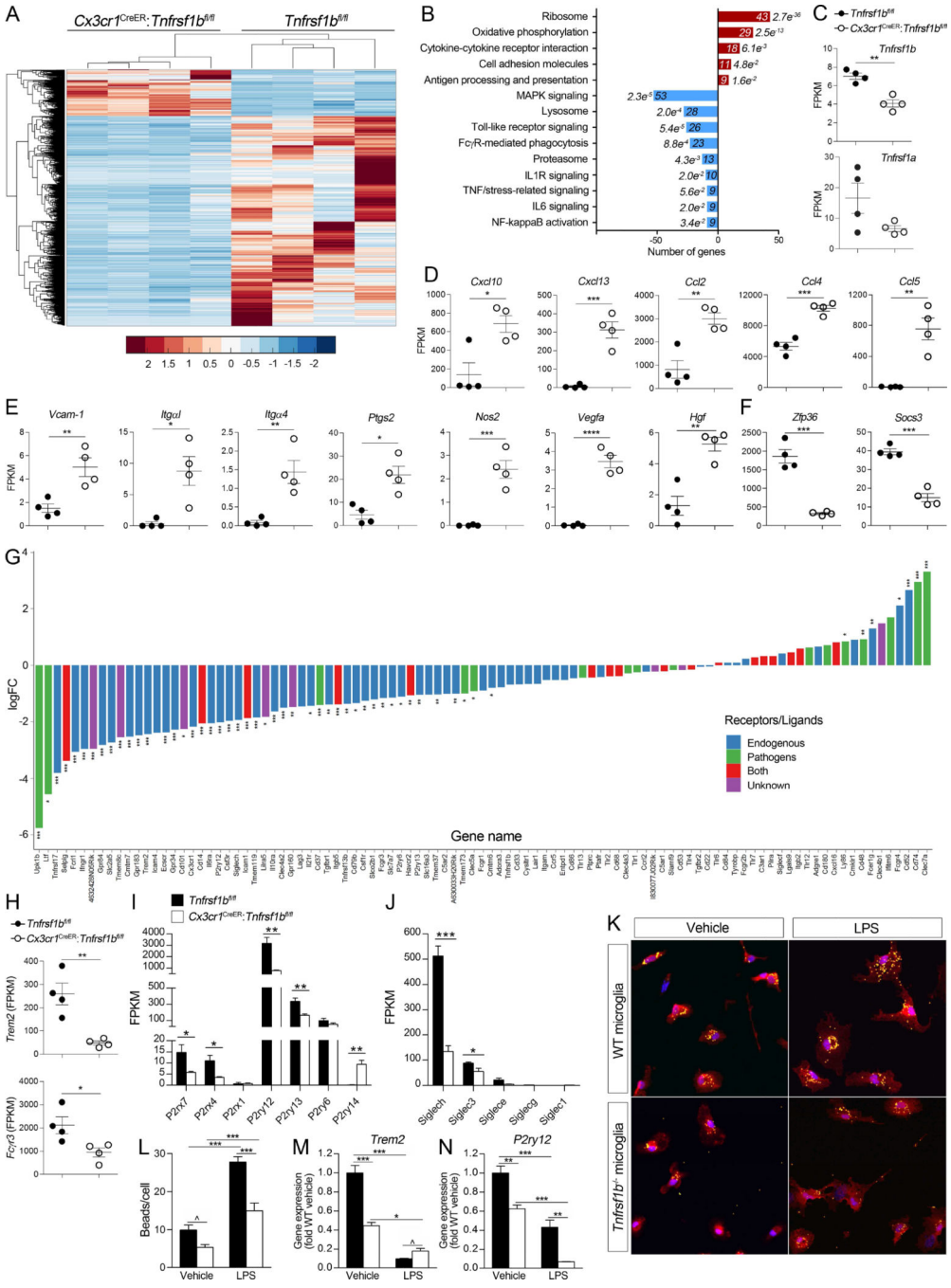

Figure 4. RNA-seq analysis of the microglial transcriptome after EAE

A) Heat map of differentially expressed genes in spinal cord microglia sorted from *Cx3cr1*$^{\text{CreER}}$:*Tnfrsf1b*$^{\text{fl/fl}}$ and *Tnfrsf1b*$^{\text{fl/fl}}$ mice at 17 dpi; n=4/group. Changes are expressed as Log_2 values. Red: upregulated genes; blue: downregulated genes. (B) DAVID pathway analysis of differentially expressed genes in *Cx3cr1*$^{\text{CreER}}$:*Tnfrsf1b*$^{\text{fl/fl}}$ vs *Tnfrsf1b*$^{\text{fl/fl}}$ mice. Red: upregulated pathways; blue: downregulated pathways. P values are shown next to the bars. (C-F, H) Expression profiles of select genes from the RNA-seq analysis shown as Fragments Per Kilobase per million Mapped reads (FPKM); *p ≤ 0.05, **p ≤ 0.01, ***p ≤

0.001, ****p ≤ 0.0001, Student's *t* test. (G) Expression of microglial sensome genes in *Cx3cr1*^{CreER}:*Tnfrsf1b*$^{fl/fl}$ vs *Tnfrsf1b*$^{fl/fl}$ mice; *p ≤ 0.05, **p ≤ 0.01, ***p ≤ 0.001, EdgeR analysis. (I, J) Expression of purinergic (I) and Siglec (J) receptors obtained from the RNA-seq analysis; *p ≤ 0.05, **p ≤ 0.01, ***p ≤ 0.001, Student's *t* test. (K, L) Quantification of microglial phagocytosis in vitro. Fluorescent beads incorporated by primary microglia from WT and *Tnfrsf1b*$^{-/-}$ mice (K) were quantified in unstimulated conditions or after LPS treatment (L); n=6/group, ***p ≤ 0.001, one-way ANOVA, Tukey test; ^p ≤ 0.05, Student's *t* test. (M, N) Expression of *Trem2* (M) and *P2ry12* (N) in cultured microglia; n=6/group, *p ≤ 0.05, **p ≤ 0.01, ***p ≤ 0.001, one-way ANOVA, Tukey test; ^p ≤ 0.05, Student's *t* test. See also Fig. S4.

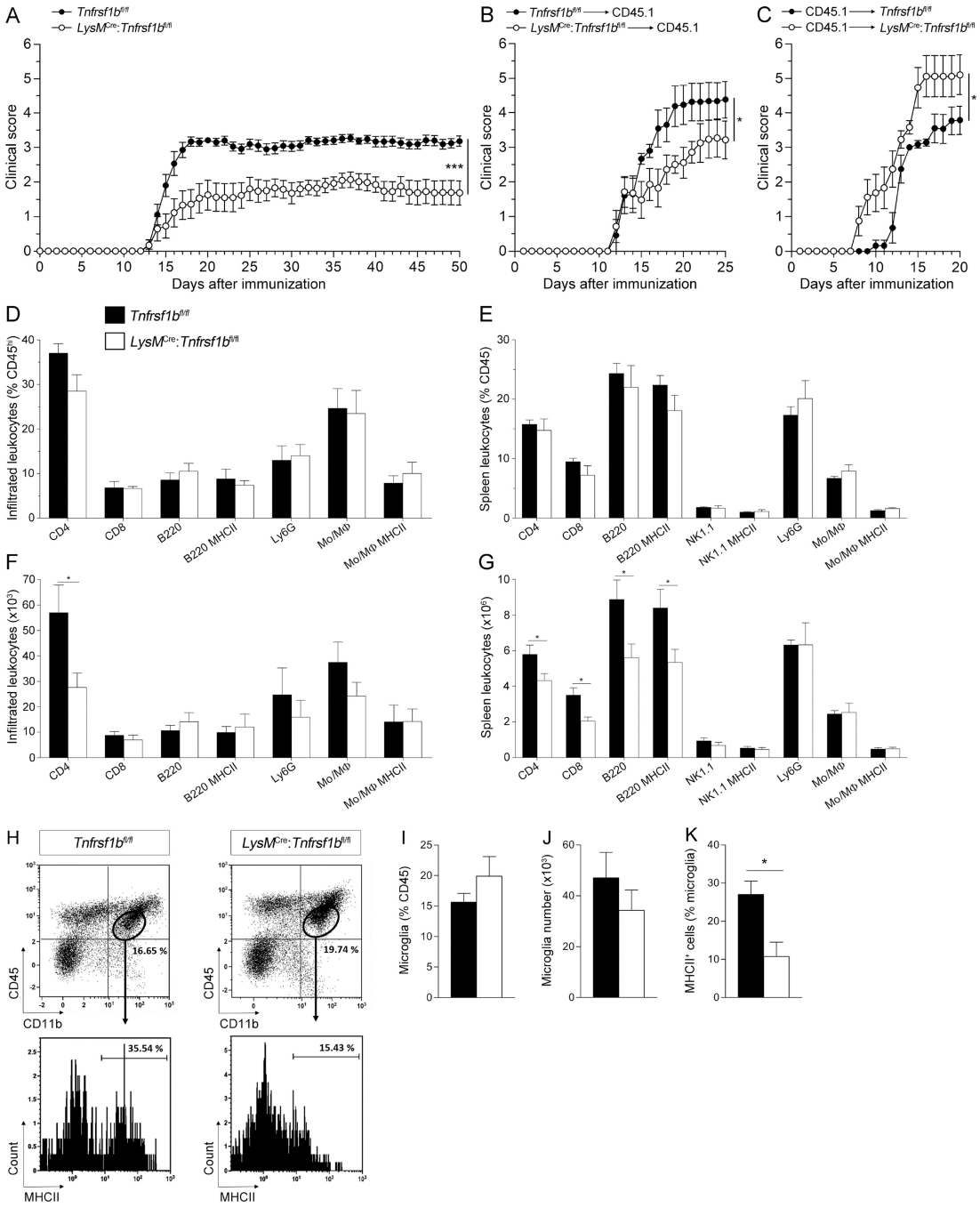

Figure 5. Ablation of TNFR2 in *LysM*^{Cre}:*Tnfrsf1b*$^{fl/fl}$ mice results in suppression of EAE

(A) Clinical course of EAE in *Tnfrsf1b*$^{fl/fl}$ and *LysM*^{Cre}:*Tnfrsf1b*$^{fl/fl}$ mice; n=12–13/group from two experiments; ***p ≤ 0.001, one-way ANOVA, Mann-Whitney test. (B, C) Clinical course of EAE in bone marrow-transplanted chimeric mice with TNFR2 ablation in Mo/MΦ [*LysM*^{Cre}:*Tnfrsf1b*$^{fl/fl}$→ CD45.1] and corresponding controls [*Tnfrsf1b*$^{fl/fl}$ → CD45.1] (B), or in microglia [CD45.1 → *LysM*^{Cre}:*Tnfrsf1b*$^{fl/fl}$] and corresponding controls [CD45.1 → *Tnfrsf1b*$^{fl/fl}$] (C); n=6–7/group, *p ≤ 0.05, one-way ANOVA, Mann-Whitney test. (D, F) Flow cytometric analysis of the frequency (D) and absolute numbers (F) of infiltrated

leukocytes at 20 dpi; n=5/group, *p ≤ 0.05, Student's *t* test. (E, G) Flow cytometric analysis of the frequency (D) and absolute numbers (F) of splenic leukocytes at 20 dpi. Mo/MΦ are defined as $CD45^{hi}CD11b^{+}NK1.1^{-}Ly6G^{-}SSA^{low}$; n=8–11/group, *p ≤ 0.05, Student's *t* test. (H) Representative flow plots of spinal cord microglia at 20 dpi. (I-K) Quantification of percentage (I) and number (J) of microglia, and percentage of $MHCII^{+}$ activated microglia (K); n=5–6/group, *p ≤ 0.05, Student's *t* test.

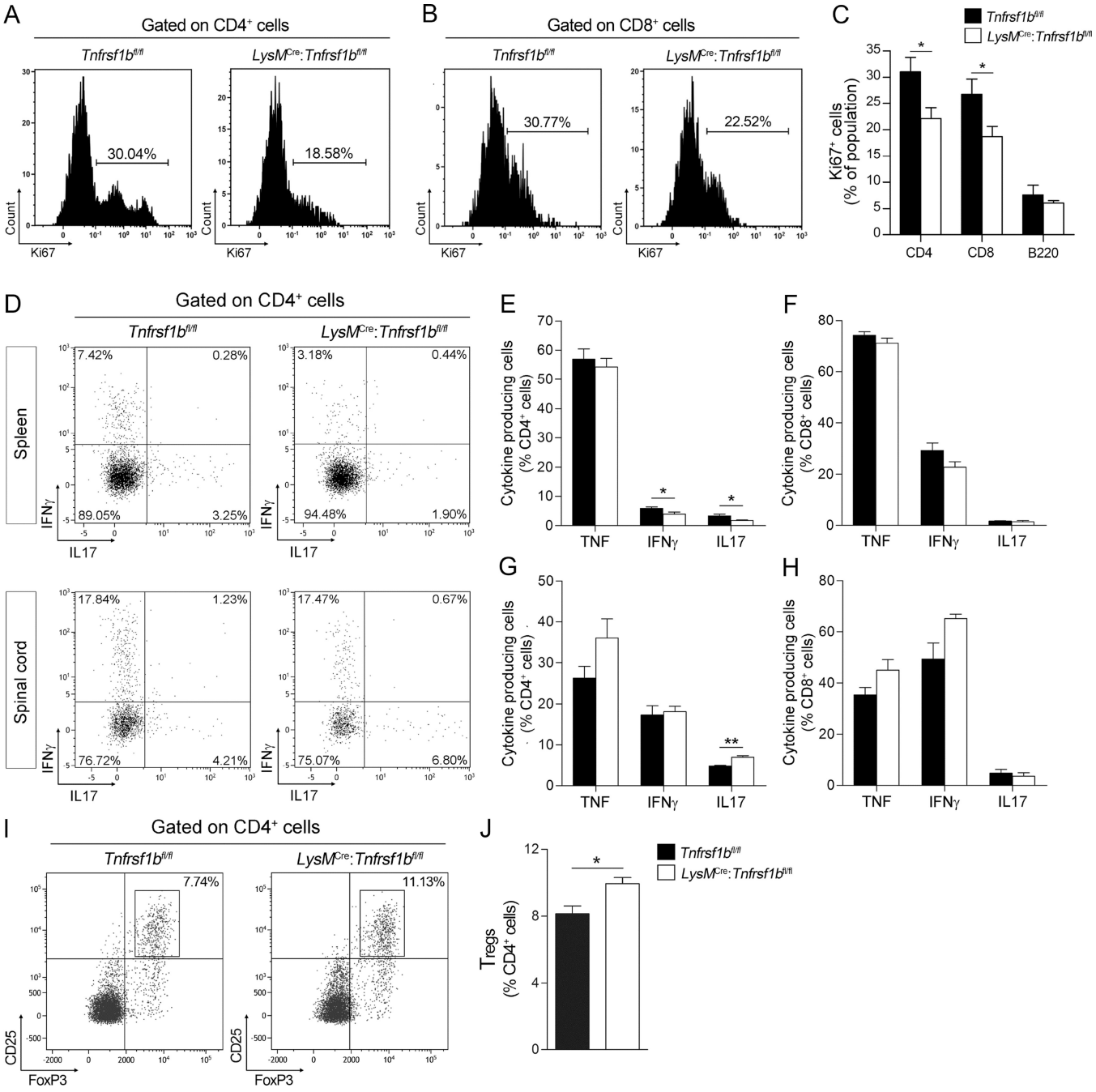

Figure 6. Ablation of TNFR2 in *LysM*^{Cre}:*Tnfrsf1b*$^{fl/fl}$ mice results in impaired T cell proliferation and effector function in the spleen after EAE

A, B) Representative flow plots of Ki67 expression in CD4 (A) and CD8 (B) T cells in *Tnfrsf1b*$^{fl/fl}$ and *LysM*^{Cre}:*Tnfrsf1b*$^{fl/fl}$ mice at 12 dpi. (C) Quantification of Ki67^{+} splenic lymphocytes; n=4–5/group, *p ≤ 0.05, Student's *t* test. (D) Representative flow plots of cytokine expression in CD4 T cells from spleen and spinal cord at 20 dpi. (E-H) Quantification of cytokine expression in CD4 and CD8 T cells; n=3–6/group, *p ≤ 0.05, **p ≤ 0.01, Student's *t* test. (I) Representative flow plots of splenic T^{regs} in *Tnfrsf1b*$^{fl/fl}$ and

LysM^{Cre}:*Tnfrsf1b*$^{fl/fl}$ mice at 20 dpi. (J) Quantification of splenic T^{reg} frequency; n=4–5/group, *$p \leq 0.05$, Student's *t* test. See also Fig. S6.

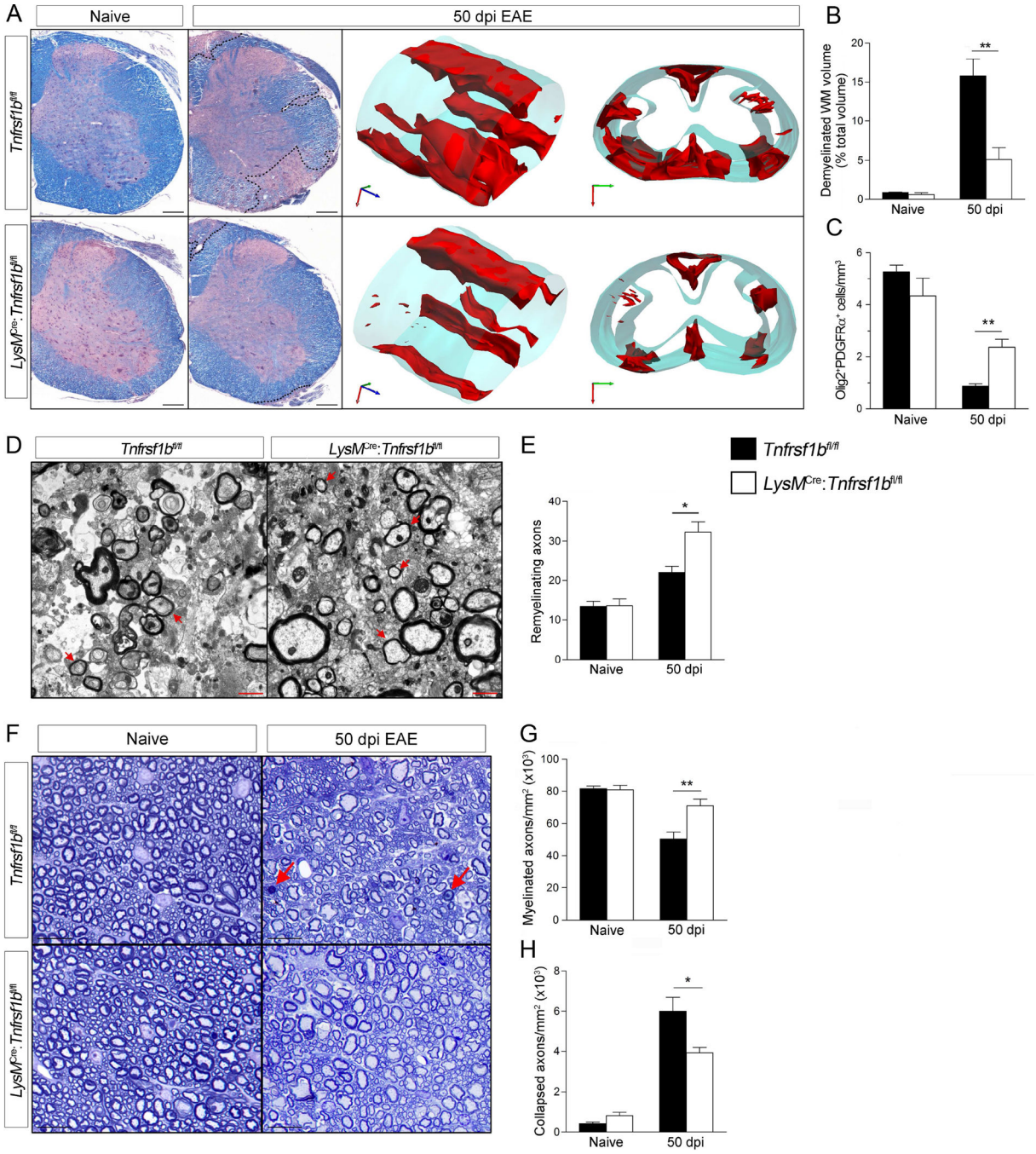

Figure 7. Ablation of TNFR2 in *LysM*^{Cre}:*Tnfrsf1b*$^{fl/fl}$ mice results in reduced demyelination and improved remyelination and neuroprotection in EAE

A) Assessment of demyelination in the spinal cord of *Tnfrsf1b*$^{fl/fl}$ and *LysM*^{Cre}:*Tnfrsf1b*$^{fl/fl}$ mice by LFB staining. Left: contoured areas show regions of demyelinated white matter; scale bar = 200 μm. Right: 3D reconstructions of the demyelinated areas (red). (B) Quantification of the demyelinated white matter volume; n=3–5/group, **p ≤ 0.01, Student's *t* test. (C) Quantification of Olig2^{+}PDGFRα^{+} OPCs in the spinal cord; n=3–5/group, **p ≤ 0.01, Student's *t* test. (D) Representative electron micrographs of the spinal cord at 50 dpi showing remyelinated axons (red arrows); scale bar: 1 μm. (E) Quantification

of remyelinated axons; n=4–5/group, *p ≤ 0.05, Student's *t* test. (F) Toluidine blue staining of spinal cord sections from naive and 50 dpi mice. Red arrows indicate degenerated axons; scale bar: 10 μm. (G, H) Quantification of myelinated (G) and degenerated (H) axons; n=4–5/group, *p ≤ 0.05, *p ≤ 0.01, Student's *t* test.